Development of a Long-Range Hydrological Drought Prediction Framework Using Deep Learning

Mohd Imran Khan[1] · Rajib Maity[1]

Abstract

Long-range (1 to 6 months in advance) prediction of droughts is challenging due to its inherent complexity. In this study, we developed a Long-Range Hydrological Drought Prediction Framework (HDPF), empowered by a Deep Learning (DL) approach. Starting with two state-of-the-art approaches, namely Long Short-Term Memory (LSTM), and one-dimensional Convolutional neural networks (Conv1D), we picked out Conv1D to develop the HDPF, being its relatively better performance. The devised HDPF leverages a comprehensive set of eight meteorological precursors, harnessing their collective potential to offer predictions of reasonable accuracy ($> 70\%$). The developed HDPF is able to extract the hidden information from the pool of meteorological precursors along with its evolution over time and influence on the upcoming drought status. Additionally, while comparing the performance of the Conv1D against LSTM, it is noticed that the performance of LSTM is at par with that of Conv1D. However, considering the model parsimony and computational time we advocate the usage of Conv1D. Moreover, comparison against other popular machine learning models, such as Support Vector Regression (SVR) and Feedforward Neural Network (FNN) further affirms the superiority as well as benefits of Conv1D. The developed HDPF can also be useful to other basins in a different climate regime, subject to its recalibration with the location-specific datasets. Overall, this study advances drought prediction methodologies by demonstrating the potential of DL techniques while underscoring the utility and adaptability of the proposed Conv1D-based HDPF.

✉ Rajib Maity
rajib@civil.iitkgp.ac.in; rajibmaity@gmail.com

[1] Department of Civil Engineering, Indian Institute of Technology Kharagpur, Kharagpur 721302, West Bengal, India

1 Introduction

Drought is one of the most severe, recurring and precarious natural disasters that affects around 55 million people every year globally (Pham et al. 2021; Poonia et al. 2021). It is typically caused by a precipitation deficiency, although temperature and evapotranspiration anomalies may also contribute (Mishra and Singh 2010). Moreover, variations in land use and land cover patterns, along with reservoir mismanagement, may further influence drought progression. Thus, drought is driven by interactions among water management, land surface processes, and climate anomalies (Hao et al. 2018).

Droughts can be broadly classified into four categories, namely meteorological, agricultural, hydrological and socio-economic droughts (Mishra and Singh 2010; Crausbay et al. 2017; Piri et al. 2023). This study focuses on hydrological droughts, which is recognized as a multifaceted phenomenon shaped by diverse hydrometeorological factors having significant impacts on water availability, power generation, water quality, riparian habitats, recreation and crop failure (Akbari et al. 2015). The critical challenge in this endeavour lies in advancing long-term predictions, a pivotal facet of effective drought management (Deo et al. 2017; Hao et al. 2018). According to Deo et al. (2017), an effective drought forecasting model consists of four fundamental components: i) selection of drought indices ii) identification of causal attributes iii) choice of model, and iv) evaluation of model outcome.

Drought modeling employs diverse approaches, with a recent focus on Machine Learning (ML) for enhanced performance (Anshuka et al. 2019; Roushangar et al. 2022; Jariwala and Agnihotri 2023). While detailed discussions about different ML models, data types, and variables used in drought-related studies can be found elsewhere (AghaKouchak et al. 2015; Hao et al. 2018; Fung et al. 2020; Dikshit et al. 2022b), forecasting drought at longer leads using ML presents challenges like dimensionality and overfitting (Deo et al. 2017; Dikshit et al. 2022b). Deep learning (DL), a new domain of ML, addresses these challenges and offers improved approaches (Reichstein et al. 2019; Latif and Ahmed 2023). Notably, Convolutional Neural Network (CNN) and Long Short-Term Memory (LSTM) neural networks have been popularly employed, demonstrating reasonably good performance in modeling hydroclimatic variables (Ham et al. 2019; Kratzert et al. 2019a, b; Duan et al. 2020; Khan and Maity 2020; Khan and Maity (2022); Lees et al. 2022). The integration of these advanced techniques holds promises for addressing the intricacies of drought forecasting at extended lead times. However, their applications in drought prediction is still in its early stages, especially in hydrological drought studies on the Indian mainland, with limited applications (Maity et al. 2021; Dikshit et al. 2022a).

In summary, most of the reviewed studies have concentrated on leveraging the capabilities of LSTM. A very limited number of DL based data-driven investigations have centred on achieving optimal computational efficiency and delving into the capabilities of a one-dimensional CNN (Conv1D) for predicting hydroclimatic variables, despite its notable performance in diverse domains. Additionally, prediction of hydrological drought using DL has not been explored, particularly in the context of the Indian mainland. In light of these arguable points, we are motivated to develop a modest and computationally efficient long-range (up to 6 months in advance) Hydrological Drought Prediction Framework (HDPF) by configuring a new Conv1D architecture using meteorological precursors. Notably, the proposed framework is aimed to harness the complex and hidden information from the pool of meteorological precursors along with its evolution over time and influence on the upcoming drought status. Furthermore, the effectiveness of the aforementioned Conv1D-based

HDPF is established by comparing its performance against three well established models, namely LSTM, Support Vector Regression (SVR), and Feedforward Neural Network (FNN) in predicting hydrological drought up to 6 months in advance.

2 Study Area and Data Used

The central Indian region spanning from the Upper Mahanadi River Basin (UMRB) to the Basantpur Gauging Station is chosen to evaluate the predictive capability of the Conv1D-based HDPF (Fig. 1). Covering 58,426 km^2, the UMRB is situated between 19.50° N to 23.50° N and 80.50° E to 83.50° E, with a topography varying from 151 to 1079 m. Experiencing four distinct seasons—winter, summer, southwest monsoon, and post-monsoon—the UMRB faces extreme climate, with summers reaching upto 50 °C and winters dropping below 10 °C. Despite an annual precipitation of 1463 mm, mainly during the southwest monsoon (June to September), the basin's uneven distribution makes it vulnerable to drought, exacerbated by climate change. The Mahanadi river is the primary watercourse of the basin flowing eastward into the Bay of Bengal. Approximately half of the basin is allocated for agriculture, relying on rain-fed rivers and groundwater (Asokan and Dutta 2008).

A set of nine hydrometeorological variables, namely total precipitation, air temperature, evaporation, surface pressure, soil water, zonal wind speed, meridional wind speed, geopotential height, relative humidity and streamflow, is used to develop the proposed HDPF. Among the listed hydrometeorological precursors, streamflow data for the Basantpur gauging station (Jan 1972 to Feb 2019) was sourced from the Water Resource Information System Portal of India (India-WRIS: https://indiawris.gov.in/wris/#/RiverMonitoring, accessed in Nov 2022). Other variables were obtained from the fifth generation of the European Centre for Medium-Range Weather Forecasts (ECMWF) reanalysis product
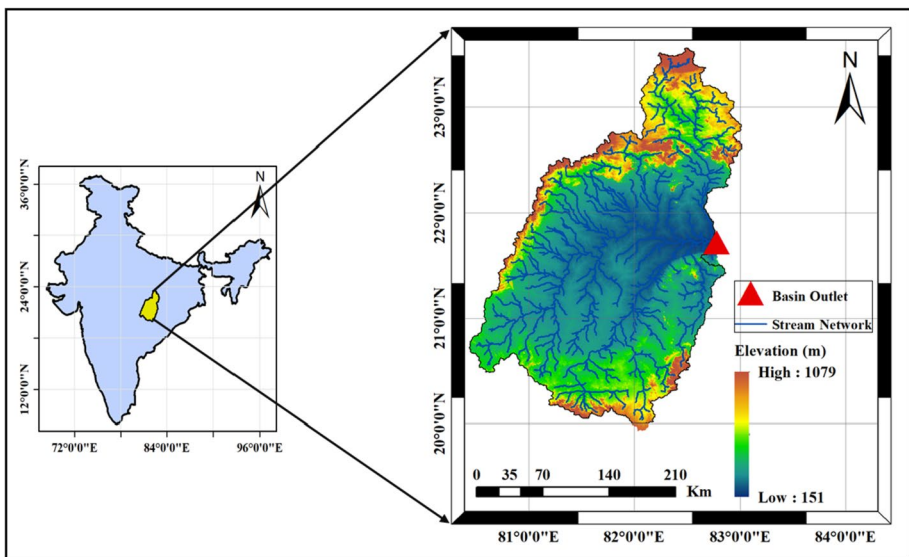

Fig. 1 Illustration of the Upper Mahanadi River Basin, along with its stream network, elevation and outlet point, located in the central belt of Indian mainland

(ERA5, https://www.ecmwf.int/en/forecasts/datasets/reanalysis-datasets/era5, accessed in Nov 2022). ERA5 is a widely used source which provides a range of atmospheric, land, and oceanic variables globally at different spatio-temporal scales (viz., spatially $0.1° \times 0.1°$ and $0.25° \times 0.25°$, temporally hourly and monthly). More specifics on dataset processing are presented in Section 3.2.

3 Methodology

A flowchart summarising the proposed HDPF built using Conv1D is shown in Fig. 2. In the following subsections, an explanation is offered explaining each element involved in the development of the framework.

3.1 Selection of Drought Index

In the field of hydrological drought research, prevalent drought indices comprises of the Palmer Hydrological Drought Index (PHDI), Standardized Streamflow Index (SSI), Standardized Runoff Index (SRI), Standardized Reservoir Supply Index (SRSI), Streamflow Drought Index (SDI) and Standardized Streamflow Anomaly Index (SSAI) (Makokha et al. 2016; Hao et al. 2018; Dutta and Maity 2021). The selection of these indices depends on the application and research area, each carrying specific advantages and disadvantages. In this study, SSAI is chosen to describe above/below-normal flow occurrences, aligning with its established robustness in the literature (Chanda and Maity 2015; Rehana and Monish 2020). The detailed procedure of calculating SSAI is provided in Supplementary Section S1.

3.2 Preparation of Dataset

Initial (raw) collection of datasets obtained from ERA5 and India-WRIS comprises of nine hydrometeorological variables as mentioned in Section 2. These organizations ensure the quality of the data before making these available (https://www.ecmwf.int/en/about/media-centre/focus/2023/fact-sheet-reanalysis, https://indiawris.gov.in/wris/#/about and https://indiawris.gov.in/downloads/Mahanadi%20Basin.pdf).
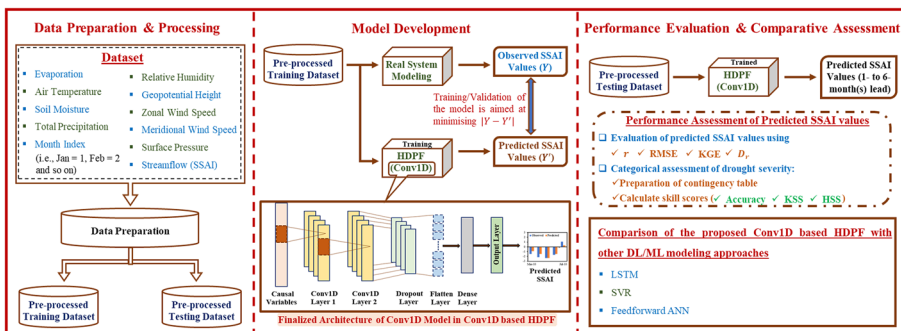

Fig. 2 An illustration of the proposed Conv1D-based Hydrological Drought Prediction Framework (HDPF)

The preparation starts with spatial averaging of the gridded data set across the selected basin by utilising the area weightage method. Next, the streamflow data, obtained at a daily scale, undergoes conversion to a monthly scale, and then to their corresponding SSAI values through the methodology outlined in Supplementary Section S1. Next, the zonal and meridional components of wind speed are converted to a single component, named resultant wind speed. In addition to the meteorological precursors, a monthly index (i.e., for Jan = 1, Feb = 2, …., and Dec = 12) for the entire period, is also added as one of the causal variables. After completion of the aforesaid tasks, a refined dataset comprising of nine variables, namely month index, total precipitation, air temperature, surface pressure, soil water, resultant wind speed, geopotential height, relative humidity and SSAI, is obtained.

Next, the variables are scaled, excluding the month index and SSAI features. In this process, the dataset is initially divided into two segments: training (80%) and testing (20%). Thereafter, the time series of the variables are subtracted from its training data mean and divided by its training data standard deviation. It may be noted here that we have selected the training dataset from January 1972 to December 2009, and the testing dataset from January 2010 to February 2019, with the intent to keep the testing period as recent as possible.

3.3 Proposed Deep Learning Model

Conv1D is a type of CNN that uses 1-dimensional convolutional operations to extract hidden, nonlinear, and complex dataset characteristics and learn causal-target association. 1D filters provide real-time, low-cost hardware implementation (Kiranyaz et al. 2019). The Conv1D model created in this study predicts SSAI values at varied lead periods.

CNN architectures typically have input layer, hidden layer(s), and output layer. The model's initial convolutional layer (i.e., the input layer) has input shape as an argument. The CNN model, specifically its Conv1D variant, requires three-dimensional tensor data (number of samples, time steps, features). Other than the input shape argument, the initial Conv1D layers have the same arguments as hidden layer ones. The number of filters, strides, kernel initializer, kernel regularizer, activation function, padding, and other hyperparameters control the computation of the Conv1D layer. Details about the function of different hyperparameters of the Conv1D layer can be found in Kiranyaz et al. (2019).

The hidden layer follows the input layer. These layers represent the model's computation engine and are problem specific i.e., their number and type are not fixed. Common hidden layers include convolutional, pooling, dropout, flatten, and dense/fully connected layers. The hidden layer(s) convolutional layer works similarly to the first layer. In a convolutional layer, the next layer's neurons are linked to an area of the preceding layer. This type of connection captures only the effective predictors of the target value, minimizing the need to investigate all characteristics, making it useful for handling large input sets. If employed, the pooling layer, another hidden layer, follows the convolutional layer. These layers reduce the preceding convolutional layer's representation scale. There are average and maximum pooling layers. Average pooling layer takes average value, while maximum pooling layer chooses greatest value in each filter-overlaid input region.

Other types of hidden layers, such as the dropout layer, help to tackle the problem of overfitting (if any) in a DL model (Srivastava et al. 2014). The flatten layer follows the last convolutional/pooling/dropout layer in Conv1D and reduces three-dimensional shape to one-dimension for the FCL. Generally, FCL is commonly used as an output layer in the Conv1D model. However, they can also be used as a hidden layer, depending on the requirements of the problem. Number of neurons in output FCL symbolizes targets.

Similar to Conv1D, FCL layers include numerous arguments, such as number of neurons, activation function, kernel initializer, kernel regularizer, etc., that affect their operation. A comprehensive explanation of the FCL layers is available in ASCE Task Committee 2000.

3.4 Performance Evaluation of the Conv1D-Based HDPF

3.4.1 Assessment of the Conv1D-Based HDPF in the Prediction of SSAI

The Conv1D-based HDPF is trained to predict 1- to 6-month(s) hydrological drought (SSAI values) simultaneously. The performance during the training and testing is assessed with the help of four popular statistical metrics: i) Coefficient of Correlation (r), ii) Root Mean Squared Error ($RMSE$), iii) Kling-Gupta Efficiency (KGE), and (iv) Refined Index of Agreement (D_r) (Pearson and Henrici 1895; Gupta et al. 2009; Willmott et al. 2012; Chai and Draxler 2014). The mathematical expressions of these metrics are provided in the Supplementary Section S2.

3.4.2 Assessment of the Conv1D-Based HDPF in the Prediction of Drought Categories

The performance of the hydrological drought category is assessed with the help of a contingency table. A typical contingency table for c × c dimension along with a detailed explanation are provided in the Supplementary Section S3.

3.4.3 Contemporary Approaches

To establish the efficacy of the proposed Conv1D-based HDPF, LSTM-based HDPF is developed to forecast the hydrological drought (upto 6 months advance) by using the same proportion of training and testing datasets as utilised in the prior case. Additionally, a comparison of the proposed framework is also made with SVR and FNN models. A detailed description of these are provided in Section 4.3.

4 Results and Discussion

4.1 Performance Assessment of the Conv1D-Based HDPF in Predicting Hydrological Drought

The developed Conv1D-based HDPF is tested to predict hydrological drought, at six consecutive leads simultaneously. A discussion about the model development process is provided in Supplementary Section S4. The predicted SSAI time series during the testing period in the case of 1-, 2-, 3-, 4-, 5- and 6-month leads lies between, Jan 2010-Feb 2019 (110 months), Feb 2010-Feb 2019 (109 months), Mar 2010-Feb 2019 (108 months), Apr 2010-Feb2019 (107 months), May 2010-Feb 2019 (106 months), Jun 2010-Feb 2019 (105 months), respectively.

Table 1 shows the performance of the Conv1D-based HDPF in terms of r, $RMSE$, KGE, and D_r, obtained for the training and testing period at the selected six leads. It can be observed in the table that model prediction efficiency (KGE) during the testing period, at 1-month lead is 79%, which is quite good. However, a decrease in KGE is noticed at longer lead, which is quite expected. The range of KGE values obtained, at various lead months

Table 1 Performance of Conv1D-based HDPF in predicting SSAI at different leads (in months) during the training (tr) and testing (ts) periods

Lead Time	Coefficient of Correlation		Root Mean Square Error		Kling Gupta Efficiency		Refined Index of Agreement	
	tr	ts	tr	ts	tr	ts	tr	ts
1 Month	0.98	0.96	0.27	0.34	0.81	0.79	0.86	0.85
2 Month	0.98	0.95	0.29	0.36	0.83	0.85	0.85	0.84
3 Month	0.96	0.95	0.27	0.37	0.81	0.74	0.88	0.84
4 Month	0.96	0.94	0.27	0.38	0.92	0.75	0.89	0.84
5 Month	0.96	0.95	0.26	0.39	0.88	0.72	0.90	0.83
6 Month	0.96	0.94	0.31	0.41	0.81	0.70	0.86	0.82

during the training and testing periods lies between 0.81 to 0.92 and 0.70 to 0.85, respectively. Likewise, the performance, evaluated in terms of the other three metrics, is also reasonably good. For instance, a range of values between 0.96 to 0.98 (*r* value), 0.26 to 0.31 (*RMSE* value), and 0.85 to 0.90 (D_r value) during training and 0.93 to 0.96 (*r* value), 0.35 to 0.42 (*RMSE* value), and 0.81 to 0.85 (D_r value) during testing is obtained. Moreover, a comparable performance during the training and testing period at each lead ensures the proper training/validation of the Conv1D model during its development and hence eradicates any doubt of overfitting/underfitting of the model.

Additionally, the performance of the proposed framework is also visualized through bar plots and scatter plots. Figure 3 illustrate these plots for the testing dataset obtained at six leads. It is noticed that the majority of the observed SSAI values, which indicates above/below-normal events, are effectively captured at a 1-month lead. However, a marginally lower performance in capturing SSAI is noticed in the advanced lead. The potential of the Conv1D in capturing the hydrological extremes is also visible in the scatter plots, shown on the right side, in Fig. 3. The marginal deviation between the 45-degree line (red colour) and the best-fit line (black colour), drawn in the scatter plot, demonstrates the efficacy of the framework at all six leads, and the same is also evident from the performance metrics shown in Table 1.

Moreover, an in-depth analysis of the Conv1D-based HDPF performance in categorizing near above/below-normal events is also carried out. An explanation of the same is provided in the following subsection.

4.2 Potential of Conv1D-Based HDPF in the Characterization of Drought Severity at Multi-Step Lead (Upto 6 Month)

A contingency table is prepared to demonstrate the effectiveness of Conv1D-based HDPF in categorizing drought severity. Figure 4 shows the contingency table, compiled using the testing performance of the proposed framework to compare the observed vs. predicted SSAI, classified into various categories based on the severity of above/below-normal flow events, at each predicted lead. It is observed that out of a total of 6 extreme dry events that occurred during each 1-, 2- and 3-month lead, the model is able to capture 4, 5, and 2 dry events in each lead respectively. The remaining events at, 1-month lead (i.e., 2 events) are classified as severe drought, 2-month lead (i.e., 1 event) is classified as moderate drought, and, 3-month lead (i.e., 4 events), 3 are classified as severe and 1 is classified as a moderate dry event(s). Likewise, during the 5- and 6-month lead prediction, out of a total of 5
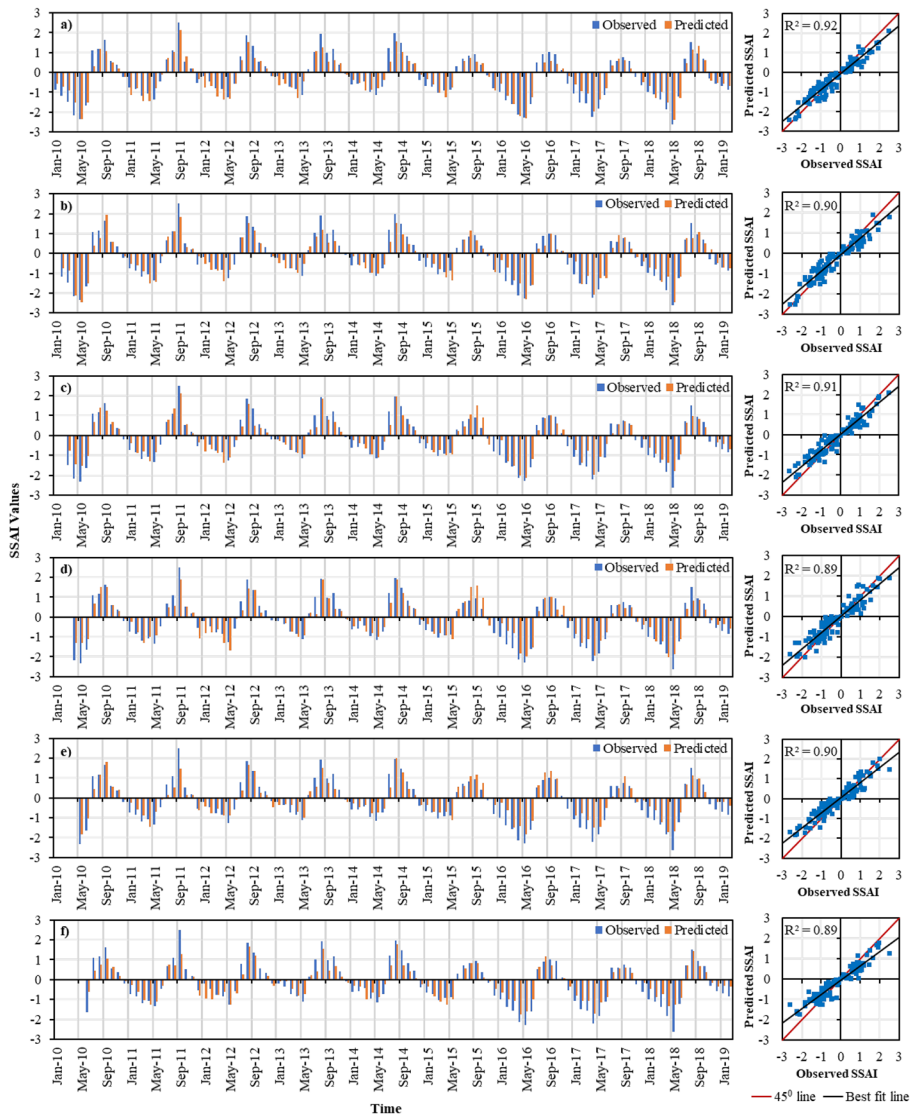
Fig. 3 Conv1D-based HDPF performance in prediction of hydrological drought, viz., **a** 1-month lead, **b** 2-month lead, **c** 3-month lead, **d** 4-month lead, **e** 5-month lead, **f** 6-month lead. Bar plots (left) and scatter plots (right) depict the observed and predicted values of SSAI at different leads during the testing period

and 4 extreme dry events that occurred, 4 were classified as severe dry and 1 as moderate dry, and 3 were classified as severe dry and 1 as moderate dry, respectively. Thus, the Conv1D-based HDPF shows a promising performance in predicting extreme dry events effectively; however, its accuracy decreases gradually with the increase in lead time.

Similar to the measure of the effectiveness of the model in categorizing extreme dry events, the *accuracy* of the proposed HDPF is also assessed in categorizing severe dry
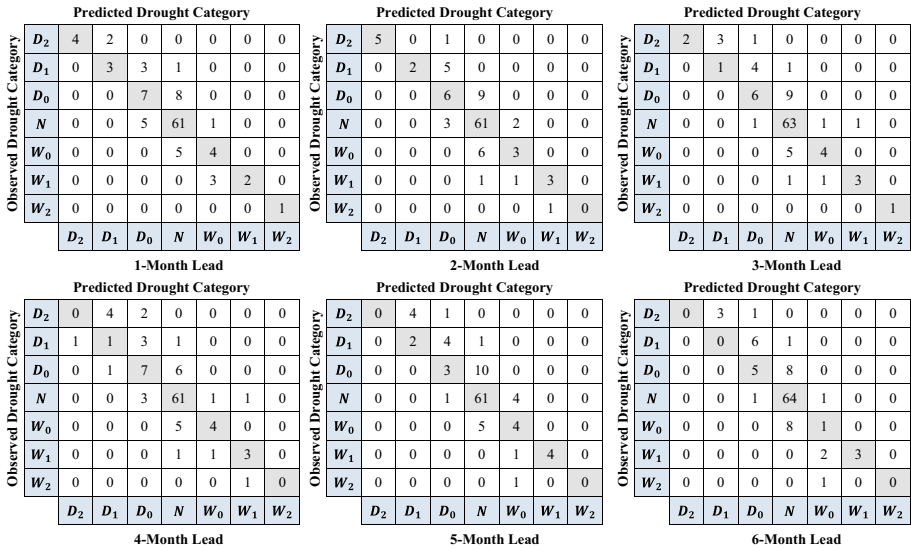
Predicted Drought Category — 1-Month Lead

Observed Drought Category	D_2	D_1	D_0	N	W_0	W_1	W_2
D_2	4	2	0	0	0	0	0
D_1	0	3	3	1	0	0	0
D_0	0	0	7	8	0	0	0
N	0	0	5	61	1	0	0
W_0	0	0	0	5	4	0	0
W_1	0	0	0	0	3	2	0
W_2	0	0	0	0	0	0	1

Predicted Drought Category — 2-Month Lead

Observed Drought Category	D_2	D_1	D_0	N	W_0	W_1	W_2
D_2	5	0	1	0	0	0	0
D_1	0	2	5	0	0	0	0
D_0	0	0	6	9	0	0	0
N	0	0	3	61	2	0	0
W_0	0	0	0	6	3	0	0
W_1	0	0	0	1	1	3	0
W_2	0	0	0	0	0	1	0

Predicted Drought Category — 3-Month Lead

Observed Drought Category	D_2	D_1	D_0	N	W_0	W_1	W_2
D_2	2	3	1	0	0	0	0
D_1	0	1	4	1	0	0	0
D_0	0	0	6	9	0	0	0
N	0	0	1	63	1	1	0
W_0	0	0	0	5	4	0	0
W_1	0	0	0	1	1	3	0
W_2	0	0	0	0	0	0	1

Predicted Drought Category — 4-Month Lead

Observed Drought Category	D_2	D_1	D_0	N	W_0	W_1	W_2
D_2	0	4	2	0	0	0	0
D_1	1	1	3	1	0	0	0
D_0	0	1	7	6	0	0	0
N	0	0	3	61	1	1	0
W_0	0	0	0	5	4	0	0
W_1	0	0	0	1	1	3	0
W_2	0	0	0	0	0	1	0

Predicted Drought Category — 5-Month Lead

Observed Drought Category	D_2	D_1	D_0	N	W_0	W_1	W_2
D_2	0	4	1	0	0	0	0
D_1	0	2	4	1	0	0	0
D_0	0	0	3	10	0	0	0
N	0	0	1	61	4	0	0
W_0	0	0	0	5	4	0	0
W_1	0	0	0	0	1	4	0
W_2	0	0	0	0	1	0	0

Predicted Drought Category — 6-Month Lead

Observed Drought Category	D_2	D_1	D_0	N	W_0	W_1	W_2
D_2	0	3	1	0	0	0	0
D_1	0	0	6	1	0	0	0
D_0	0	0	5	8	0	0	0
N	0	0	1	64	1	0	0
W_0	0	0	0	8	1	0	0
W_1	0	0	0	0	2	3	0
W_2	0	0	0	0	1	0	0

Fig. 4 The compilation of contingency tables at six leads are shown to compare the observed vs. predicted SSAI, classified into various categories based on the severity of the flow events. The tables illustrate seven categories: namely, near-normal (N) i.e. $[-1, 1]$, moderately dry (D_0) i.e. [-1.5,-1) and moderately wet (W_0) i.e. (1,1.5], severely dry (D_1) i.e. [-2,-1.5) and severely wet (W_1) i.e. (1.5,2], extremely dry (D_2) i.e. < -2 and extremely wet (W_2) i.e. > 2. These tables assess the effectiveness of the Conv1D-based HDPF in capturing these categories

(D_1), moderate dry (D_0), normal (N), moderate wet (W_0), severe wet (W_1) and extreme wet (W_2) events accurately at 1-, 2-, 3-, 4-, 5-, and 6-month lead (Fig. 4). Overall, in general, from Fig. 4, it can be concluded that the contingency tables at all the leads have a large forward diagonal, which implies that above/below-normal flow event category classification during the testing period of the proposed Conv1D-based HDPF is reasonably accurate.

In fact, 82 out of 110 (75%) at 1-month lead, 80 out of 109 (73%) at 2-month lead, 80 out of 108 (74%) at 3-month lead, 76 out of 107 (71%) at 4-month lead, 74 out of 106 (70%) at 5-month lead and 73 out of 105 (70%) at 6-month lead are accurately predicted by the proposed HDPF. It is further noticed that Conv1D-based HDPF performance at longer leads is reduced towards both sides of high extremes, i.e., at D_2, W_2, whereas for lower extreme categories (wet and dry), the performance is reasonably good, even at higher leads. In other words, it can be said that the model is not biased towards any specific side of the extreme. Moreover, the above/below-normal flow event category classification performed by the Conv1D-based HDPF is also analysed in terms of KSS and HSS scores. These scores are also estimated from the contingency table (Fig. 4) with the help of mathematical formulas provided in Supplementary Section S3. The *KSS* and *HSS* scores for 1- to 4-month leads are reasonably good and are greater than 0.43. However, similar to the performance of other metrics, a decrease in *KSS* and *HSS* scores are also observed with advancing lead, although the scores are greater than 0.33 (*KSS*) and 0.38 (*HSS*) even at a 6-month lead.

Overall, from the aforesaid discussion of prediction of hydrological extremes (both dry and wet events), in terms of skill scores, viz., *accuracy*, *KSS* and *HSS*, and metrics,

r, *RMSE*, *KGE*, and D_r, it can be concluded that the proposed Conv1D-based HDPF performance is reasonably good.

4.3 Comparison of Conv1D-Based HDPF with LSTM, SVR and FNN Based Framework

In this section, the performance of Conv1D-based HDPF is benchmarked against three well-established models, namely LSTM, FNN and SVR. The details about the same are discussed below.

Firstly, an LSTM-based HDPF is developed to predict SSAI values 6 months in advance, utilising the same proportion of training and testing datasets as employed in the proposed framework. A detailed description of LSTM model development is provided in Supplementary Section S5.

Supplementary Table S4 shows the performance of LSTM-based HDPF during the training and testing period in terms of r, *RMSE*, *KGE*, and D_r. Analysis of Table S4 indicates that LSTM's predictive efficiency (*KGE*) consistently falls within the range of 0.81 to 0.91 during the training period and 0.70 to 0.86 during testing, across all lead times. Similarly, the performance metrics r, *RMSE*, and D_r exhibit values between 0.96 to 0.98, 0.94 to 0.97, and 0.85 to 0.90 during training, and 0.94 to 0.97, 0.36 to 0.42, and 0.81 to 0.89 during testing, respectively. The observed range of metric values suggests that the LSTM framework is also reasonably effective in predicting hydrological drought at lead times ranging from 1 to 6 months.

Next, the performance of the proposed Conv1D- and LSTM-based HDPFs is compared. To facilitate this comparison, the performance metrics of Conv1D-based HDPF (in bold) are also provided in Supplementary Table S4. From the table it can be observed that the performance of both frameworks is comparable across all the leads. However, from the model configuration and computational aspects, it is observed that LSTM model has a greater number of trainable parameters and takes more time to train on a defined set of hyperparameters. Supplementary Table S5 illustrates the summary of the Conv1D and LSTM models' parameters of each layer utilized in the prediction of hydrological drought. Due to the presence of fewer trainable parameters in the computational engine (Conv1D layers) of the proposed framework model, the execution time is almost five times faster than the LSTM. Moreover, the optimized architecture of the Conv1D model is little deeper (6 layers) than the LSTM model (4 layers), but still the computational time is less (Supplementary Table S5). The execution time mentioned in this table are specifically the time taken by the model to get trained and validated with a finalized set of hyperparameters. To finalize a single set of hyperparameters, many such runs are required. Therefore, the shorter the execution time of one run, the faster will be the grid search of hyperparameters and subsequently the finalization of the model architecture.

Before concluding, the performance of the proposed Conv1D-based HDPF is also compared with FNN and SVR. However, the respective performance of these approaches is sourced from a prior study conducted by Dutta and Maity (2021). In this study, hydrological drought forecast for the same basin, using SSAI values and a similar time length and set of meteorological precursors, is carried out at a 1- to 3-month lead. The FNN and SVR models developed by the authors are time-varying as well as time invariant models, and the results presented are for a testing period spanning between 2001 and 2018. The model's performance is assessed in two ways: a) by analysing the monthly series of the dataset and, b) considering all months as a single series. Supplementary Table S6 presents the performance of the SVR and FNN models when considering all months as a single series at

1- and 3-month leads, along with the performance of Conv1D at the same leads. The table reveals that the performance of the SVR and FNN models, measured in terms of r, *RMSE*, *NSE* and D_r, is at subpar as compared to proposed framework's model.

5 Conclusions

In this study, we introduce a DL based computational framework, named as Conv1D-based HDPF, which acts as an efficient tool in performing long lead prediction of hydrological drought (up to 6 months at a monthly scale). The developed HDPF is able to provide more than 70% accuracy even at 6-month lead, indicating its capability of extracting the complex and hidden information from the pool of meteorological precursors along with its evolution over time and influence on the upcoming drought status. Notably, the improved efficiency is also due to the optimal computational efficiency that is achieved through rigorous estimation and evaluation of hyperparameters. Moreover, the performance of the proposed methodology is benchmarked against three well-established models: LSTM, FNN and SVR to prove HDPF's benefits and efficacy.

Overall, this study makes a significant contribution to hydroclimatic research by introducing the Conv1D-based HDPF for long-lead hydrological drought prediction, paving the way for further advancements in the field. The capability to forecast long-term hydrological drought has practical implications across various sectors, including water resource management, agricultural planning, and drought assessment and preparedness. It is essential to highlight that when extending the application of the proposed framework to other basins, careful consideration of the unique characteristics and hydrometeorological precursors of the target basin during model re training and validation, to update parameters and hyperparameters, is crucial. Since the model has been rigorously trained and validated for an Indian basin, updating parameters and hyperparameters for application to other basins lying in the Indian mainland is comparatively straightforward. Furthermore, the prospect of conducting multi-basin assessments of hydrological drought using a unified modelling framework is kept as a future scope for this study.

Data Availability The data that support the findings of this study are available from: https://www.ecmwf.int/en/forecasts/datasets/reanalysis-datasets/era5, and https://indiawris.gov.in/wris/#/RiverMonitoring. The datasets are freely available and was accessed by the authors in November 2022.

Code Availability The codes required for the analysis are written in python using scientific python development environment (spyder) IDE. The codes may be available on request from the authors.

Declarations

Conflicts of Interest/Competing Interests The authors have no relevant financial or non-financial interests to disclose.

References

AghaKouchak A, Farahmand A, Melton FS et al (2015) Remote sensing of drought: Progress, challenges and opportunities. Rev Geophys 53:452–480. https://doi.org/10.1002/2014RG000456

Akbari H, Rakhshandehroo GR, Sharifloo AH, Ostadzadeh E (2015) Drought analysis based on standardized precipitation index (SPI) and streamflow drought index (SDI) in Chenar Rahdar River Basin, Southern Iran. Proc Watershed Manag Symp Am Soc Civ Eng 11–22. https://doi.org/10.1061/9780784479322.002

Anshuka A, van Ogtrop FF, Willem Vervoort R (2019) Drought forecasting through statistical models using standardised precipitation index: a systematic review and meta-regression analysis. Nat Hazards 97:955–977. https://doi.org/10.1007/s11069-019-03665-6

ASCE Task Committee (2000) Artificial neural networks in hydrology. I: Preliminary concepts. J Hydrol Eng 5:115–123

Asokan SM, Dutta D (2008) Analysis of water resources in the Mahanadi River Basin, India under projected climate conditions. Hydrol Process 22:3589–3603. https://doi.org/10.1002/hyp

Chai T, Draxler RR (2014) Root mean square error (RMSE) or mean absolute error (MAE)? -Arguments against avoiding RMSE in the literature. Geosci Model Dev 7:1247–1250. https://doi.org/10.5194/gmd-7-1247-2014

Chanda K, Maity R (2015) Meteorological drought quantification with standardized precipitation anomaly index for the regions with strongly seasonal and periodic precipitation. J Hydrol Eng 20:06015007. https://doi.org/10.1061/(asce)he.1943-5584.0001236

Crausbay SD, Ramirez AR, Carter SL et al (2017) Defining ecological drought for the twenty-first century. Bull Am Meteorol Soc 98:2543–2550. https://doi.org/10.1175/BAMS-D-16-0292.1

Deo RC, Kisi O, Singh VP (2017) Drought forecasting in eastern Australia using multivariate adaptive regression spline, least square support vector machine and M5Tree model. Atmos Res 184:149–175. https://doi.org/10.1016/j.atmosres.2016.10.004

Dikshit A, Pradhan B, Assiri ME et al (2022a) Solving transparency in drought forecasting using attention models. Sci Total Environ 837:155856. https://doi.org/10.1016/j.scitotenv.2022.155856

Dikshit A, Pradhan B, Santosh M (2022b) Artificial neural networks in drought prediction in the 21st century–A scientometric analysis. Appl Soft Comput 114:108080. https://doi.org/10.1016/j.asoc.2021.108080

Duan S, Ullrich P, Shu L (2020) Using convolutional neural networks for streamflow projection in California. Front Water 2:1–19. https://doi.org/10.3389/frwa.2020.00028

Dutta R, Maity R (2021) Time-varying network-based approach for capturing hydrological extremes under climate change with application on drought. J Hydrol 603:126958. https://doi.org/10.1016/j.jhydrol.2021.126958

Fung KF, Huang YF, Koo CH, Soh YW (2020) Drought forecasting: A review of modelling approaches 2007–2017. J Water Clim Chang 11:771–799. https://doi.org/10.2166/wcc.2019.236

Gupta HV, Kling H, Yilmaz KK, Martinez GF (2009) Decomposition of the mean squared error and NSE performance criteria: Implications for improving hydrological modelling. J Hydrol 377:80–91. https://doi.org/10.1016/j.jhydrol.2009.08.003

Ham Y, Kim J, Luo J et al (2019) Deep learning for multi-year ENSO forecasts. Nature 573:567–572. https://doi.org/10.1038/s41586-019-1559-7

Hao Z, Singh VP, Xia Y (2018) Seasonal drought prediction: Advances, challenges, and future prospects. Rev Geophys 56:108–141. https://doi.org/10.1002/2016RG000549

Jariwala KA, Agnihotri PG (2023) Comparative analysis of drought modeling and forecasting using soft computing techniques. Water Resour Manag. https://doi.org/10.1007/s11269-023-03642-6

Khan MI, Maity R (2020) Hybrid deep learning approach for multi-step-ahead daily rainfall prediction using GCM simulations. IEEE Access 8:52774–52784. https://doi.org/10.1109/ACCESS.2020.2980977

Khan MI, Maity R (2022) Hybrid deep learning approach for multi-step-ahead prediction for daily maximum temperature and heatwaves. Theor Appl Climatol 149:945–963 (2022). https://doi.org/10.1007/s00704-022-04103-7

Kiranyaz S, Avci O, Abdeljaber O, et al (2021) 1D convolutional neural networks and applications: A survey. Mech Syst Signal Process 151:1–21. https://doi.org/10.1016/j.ymssp.2020.107398

Kratzert F, Klotz D, Herrnegger M et al (2019a) Toward improved predictions in ungauged basins: Exploiting the power of machine learning. Water Resour Res 55:11344–11354. https://doi.org/10.1029/2019WR026065

Kratzert F, Klotz D, Shalev G et al (2019b) Towards learning universal, regional, and local hydrological behaviors via machine learning applied to large-sample datasets. Hydrol Earth Syst Sci 23:5089–5110. https://doi.org/10.5194/hess-23-5089-2019

Latif SD, Ahmed AN (2023) Streamflow prediction utilising deep learning and machine learning algorithms for sustainable water supply management. Water Resour Manag 37:3227–3241. https://doi.org/10.1007/s11269-023-03499-9

Lees T, Reece S, Kratzert F et al (2022) Hydrological concept formation inside long short-term memory (LSTM) networks. Hydrol Earth Syst Sci 26:3079–3101. https://doi.org/10.5194/hess-26-3079-2022

Maity R, Khan MI, Sarkar S et al (2021) Potential of deep learning in drought assessment by extracting information from hydrometeorological precursors. J Water Clim Chang. https://doi.org/10.2166/wcc.2021.062

Makokha GO, Wang L, Zhou J et al (2016) Quantitative drought monitoring in a typical cold river basin over Tibetan Plateau: An integration of meteorological, agricultural and hydrological droughts. J Hydrol 543:782–795. https://doi.org/10.1016/j.jhydrol.2016.10.050

Mishra AK, Singh VP (2010) A review of drought concepts. J Hydrol 391:202–216. https://doi.org/10.1016/j.jhydrol.2010.07.012

Pearson K (1895) Mathematical contributions to the theory of evolution-III. Regression, heredity, and panmixia. Philos Trans R Soc A Math Phys Eng Sci 187:253–318. https://doi.org/10.1098/rsta.1896.0007

Pham QB, Yang TC, Kuo CM et al (2021) Coupling singular spectrum analysis with least square support vector machine to improve accuracy of SPI drought forecasting. Water Resour Manag 35:847–868. https://doi.org/10.1007/s11269-020-02746-7

Piri J, Abdolahipour M, Keshtegar B (2023) Advanced machine learning model for prediction of drought indices using hybrid SVR-RSM. Water Resour Manag 37:683–712. https://doi.org/10.1007/s11269-022-03395-8

Poonia V, Goyal MK, Gupta BB et al (2021) Drought occurrence in different river basins of India and blockchain technology based framework for disaster management. J Clean Prod 312:127737. https://doi.org/10.1016/j.jclepro.2021.127737

Rehana S, Monish NT (2020) Characterization of regional drought over water and energy limited zones of india using potential and actual evapotranspiration. Earth Sp Sci 7:e2020EA001264. https://doi.org/10.1029/2020EA001264

Reichstein M, Camps-Valls G, Stevens B et al (2019) Deep learning and process understanding for data-driven Earth system science. Nature 566:195–204. https://doi.org/10.1038/s41586-019-0912-1

Roushangar K, Ghasempour R, Alizadeh F (2022) Uncertainty assessment of the integrated hybrid data processing techniques for short to long term drought forecasting in different climate regions. Water Resour Manag 36:273–296. https://doi.org/10.1007/s11269-021-03027-7

Srivastava N, Hinton G, Krizhevsky A et al (2014) Dropout: a simple way to prevent neural networks from overfitting. J Mach Learn Res 15:1929–1958. https://doi.org/10.1109/ICAEES.2016.7888100

Willmott CJ, Robeson SM, Matsuura K (2012) A refined index of model performance. Int J Climatol 32:2088–2094. https://doi.org/10.1002/joc.2419